Journal of Statistical Physics, Vol. 54, Nos. 1/2, 1989

Stochastic versus Chaotic Dynamics in a Deterministic System

E. Gudowska-Nowak,[1] A. Kleczkowski,[1] and G. O. Williams[2]

Received May 16, 1988

We analyze a dynamical system whose time evolution depends on an externally controlled model parameter. We observe that the introduction of state-dependent perturbations induces a variety of phenomena which can have either a chaotic or stochastic nature. We analyze the sensitivity of the dynamics and the underlying attractors to the strength, frequency, and time correlations of the external perturbations.

KEY WORDS: Chaos; noise-induced transitions; state-dependent perturbations.

1. INTRODUCTION

Many stochastic models evolving in discrete time have the structure

$$z_{k+1} = f(z_k, s_k) + \xi_k, \qquad k = 0, 1, 2, \ldots \tag{1.1}$$

The process variable z_{k+1} at time t_{k+1} is assumed to be influenced by two types of forces—the first contribution depends on the current state variable z_k and other systematically or randomly varying external parameters s_k, the effect of which can be temporally correlated, while the second contribution is commonly taken to be a noise perturbation ξ_k viewed as an average over the fast variables.

Relevant examples are to be found in genetic modeling,[1,2] where the process variable z_{k+1} represents the number of some particular species present in the model system at the begining of generation $k+1$. In

[1] Institute of Physics, Jagellonian University, 30-059 Kraków, ul. Reymonta 4, Poland.
[2] Department of Chemistry, State University of New York at Stony Brook, Stony Brook, New York 11794-3400.

0022-4715/89/0100-0539$06.00/0

ecological models, the $\{s_k\}$ are sometimes referred to as stochastic (or deterministic) environmental effects, while the $\{\xi_k\}$ are regarded as sampling or demographic effects.[3]

One of the most popular genetic models[2,3] is the mapping

$$z_{k+1} = \alpha z_k (1 - z_k) \tag{1.2}$$

which describes, for example, the spreading of an arbitrarily chosen gene in a haploid population over a sequence of generations under the influence of a systematic "selection pressure" of strength α acting on the system. Equation (1.2) defines the logistic map whose well-known properties[4] depend on the value of the single external parameter α.

A population structure can also be affected by mutations, which is reflected in the possibility of the "type" of an individual being altered as it is replaced over the course of time. Specifically, formulation of a model system in terms of a Markov chain[3] leads to the following structure for the transition probability that there will be m genes of type A, say, observed in generation $k+1$, given that there were n genes of type A present in the kth generation:

$$p_{mn} = \binom{N}{m} p_n^m (1 - p_n)^{N-m} \tag{1.3}$$

where

$$p_n = \frac{(1+\alpha/2)[x(1-\psi)+(1-x)\phi]}{(1+\alpha/2)[x(1-\psi)+(1-x)\phi]+(1-\alpha/2)[\psi x+(1-x)(1-\phi)]} \tag{1.4}$$

Here, ϕ and ψ express the respective probabilities per generation of an A type mutating to an $\bar{A}$ type and an $\bar{A}$ type mutating to an A type. The fact that one allele is better adapted to the environment than the other is reflected by the selection coefficient α. The total population of N genes remains constant in time, while the fraction of genes of type A present in the kth generation is denoted by $x = n/N$, $x \in [0, 1]$.

The continuous version of this model Markov chain converges to a diffusion process[3] whose stationary probability distribution $p_s(x, \infty)$ reveals features characteristic of noise-induced transitions.[5]

In the present paper, we adopt a picture of evolution in which the time scales of the mutation and selection processes are well separated. By assuming a symmetric model, $\psi = \phi = 1/2$, we arrive at the following difference equation describing the fluctuation in the fraction of A-type genes from one generation to the next[3,5]

$$\Delta x(t) = \frac{1}{2} - x(t) + \frac{\alpha_t x(t)[1 - x(t)]}{1 - \alpha_t/2 + \alpha_t x(t)} \tag{1.5}$$

where α_t is the selection coefficient per generation. For $\alpha_t \ll 1$, Eq. (1.5) reduces to

$$dx/dt = 1/2 - x(t) + \alpha_t x(t)[1 - x(t)] \tag{1.6}$$

If the environment exhibits a certain random variability, α_t will fluctuate from generation to generation. Such a perturbation can then be closely related to the kinetics of $x = n/N$ given by the stroboscopic map,

$$dx/dt = 1/2 - x + g(x) \sum_{k=0}^{\infty} \delta(t - k\Delta)\alpha_k \tag{1.7}$$

$$g(x) = x(1 - x) \tag{1.8}$$

where the sequence of "perturbation terms" of strength α_k represents the environmental effects leading to an incident variation of α,[6] and approximates natural noise:

$$\alpha_t = \alpha_0 + \sum_k \alpha_k \, \delta(t - k\Delta) \tag{1.9}$$

$$\alpha_0 = 0 \tag{1.10}$$

A discretized version of Eq. (1.7) can be represented by

$$x_{k+1} = \tfrac{1}{2} + e^{-\tau}(x_k - \tfrac{1}{2}) + \alpha_{k+1}\{\tfrac{1}{4} - (x_k - \tfrac{1}{2})^2 e^{-2\tau}\} \tag{1.11}$$

where $\tau = t_k - t_{k-1}$, $x_k = x(t_k + 0)$, and the interpretation of $\delta(t)$ follows Ito's rule.[6,23] The parameter α enters into Eq. (1.11) as an independent variable whose time variations are governed by some dynamics,

$$d\alpha_t = A(\alpha_t)\, dt + dS_\tau(t) \tag{1.12}$$

and we assume

$$S_\tau(t) = \tau^{1/2} \sum_{k=0}^{\lfloor t/\tau \rfloor} \eta_k \tag{1.13}$$

$A(\alpha)$ is a deterministic force exerted on α (it therefore stands for the systematic changes of α_t in the course of evolution) and $dS_\tau(t)$ reflects the presence of random external noise $\{\eta_k\}$.

In this approach, the time variations of α can be understood as the motion of a Brownian particle whose dynamics is perturbed by a random force $dS_\tau(t)/dt$. The similarity of Eqs. (1.12) and (1.13) to a Langevin equation is not purely coincidental. In fact, the solution of Eq. (1.11) can

be presented[7] as $\alpha(t) = g(t - n\tau, \alpha_n)$, where $n = \lfloor t/\tau \rfloor$, and α_n is obtained by the recursion

$$y_{n+1} = \mathbf{T} y_n \tag{1.14}$$

$$\alpha_{n+1} = g(\tau, \alpha_n) + \tau^{1/2} f(y_{n+1}) \tag{1.15}$$

$$f(\mathbf{T}^n(y)) = \eta_n(y) \tag{1.16}$$

$\mathbf{T}$ is assumed to be a measure-preserving mapping fulfilling the so-called condition of ϕ-mixing,[7,8] which expresses the asymptotic independence of events. For a real-valued function f satisfying

$$E[f] \equiv 0 \tag{1.17}$$

$$\mathrm{Var}[f] < \infty \tag{1.18}$$

with respect to the invariant measure μ of the map $\mathbf{T}$, the sum (1.13) converges to a normalized Wiener process[7-9]

$$S_\tau(t) \to \sigma W(t), \qquad \tau \to 0 \tag{1.19}$$

An illustrative example is the particular choice of $\mathbf{T}$ studied by Beck and Roepstorff[7]:

$$y_{n+1} = 2y_n^2 - 1 \tag{1.20}$$

$$\alpha_{n+1} = \lambda \alpha_n + y_{n+1}, \qquad y \in [-1, 1] \tag{1.21}$$

In the limit $\lambda = e^{-\gamma\tau} \to 1$, the system (1.20)–(1.21) is dynamically equivalent to a Langevin equation:

$$d\alpha(t) = -\gamma\alpha(t)\, dt + dS_\tau(t) \tag{1.22}$$

$$S_\tau(t) = \sigma W(t), \qquad \sigma^2 = 1/2 \tag{1.23}$$

i.e., the dynamics of α, in the limit $\tau \to 0$, are described by an Ornstein–Uhlenbeck (OU) process with correlation time $\tau_{\mathrm{corr}} = 1/\gamma$.

It should be stressed, however, that there exists a broader class of dynamic mappings $\mathbf{T}$ which will fulfill the convergence (1.19) under the conditions mentioned earlier. The logistic map serves here as a particular example of special simplicity with the properties necessary for the assertion of the theorem (1.19).

In this context, our program is to investigate the long-time predictions of the model system (1.11) in the presence of external perturnations superimposed on the parameter α.

Particular attention is focused on the class of phenomena induced by

the presence of regular perturbations (1.20)–(1.21) which converge in the limit $\lambda \to 1$ to a stationary diffusion-like stochastic process.

In Section 2, we discuss the properties of the model system in its continuous version. The deterministic analysis of the discretized equations (1.11), (1.20), and (1.21) is presented in Section 3. Studies on the stochastic nature of the external perturbations (1.20) and (1.21) are briefly reported in Section 3.1, whereas their effects on the evolution of the system are examined in Section 3.2. That section is also devoted to an analysis of some features of chaos revealed by the model dynamics. A summary of our results and a discussion are offered in Section 4.

2. CONTINUOUS VERSION OF THE MODEL DYNAMICS: LONG-TIME PREDICTIONS

In this section, we present an overview of our basic model (1.6), which can be used to describe the mechanism of genetic selection in population dynamics. Similar equations are also known to model oxidation of hemoglobin,[10] relaxation kinetics of the denaturization of DNA,[11] and chemical isomerization on surfaces.[12] The common characteristic of these phenomena is kinetics given by a second-order polynomial in a state variable parametrized by constants describing couplings to the environment.

Let us assume that in a phenomenological equation of the form (1.6) the time variability of α_t can be modeled by a stationary random process. If α_t can be viewed as the cumulative effect of a large number of small additive contributions, then by invoking the central limit theorem one can assume that α_t is Gaussian. The particular choice of the stationary Gaussian diffusion process

$$d\alpha_t = -\gamma\alpha_t\, dt + \sigma\gamma^{1/2}\, dW_t \tag{2.1}$$

leads in the limit $\gamma \to \infty$ ($\tau_{\text{corr}} = 1/\gamma \to 0$) to a "noise-induced transition"[5] at a point

$$\sigma_{\text{cr}} = 4(1 - 1/\gamma) \tag{2.2}$$

Only if $\tau_{\text{corr}} = 0$ does the collective effect of α_t describe a white noise process whose imposition on x_t transforms it into a stochastic diffusion (i.e., continuous-time Markov process). A nonvanishing τ_{corr} leads to non-Markovian dynamics of x_t, given [see (1.6)] by the equation

$$dx_t = (\tfrac{1}{2} - x_t)\, dt + E[\alpha_t]\, x_t(1 - x_t)\, dt + \alpha_t\gamma^{1/2}x_t(1 - x_t)\, dt \tag{2.3}$$

Critical behavior of this model is observable as a qualitative change in the

shape of the stationary probability distribution function $p_s(x)$ of the process x_t, which, for $\sigma > \sigma_{cr}$, becomes double peaked about a deterministically unpredictable steady state. Appearance of the new extrema of $p_s(x)$ results directly from the coupling of the system to an external noise and is commonly treated as an operational test for the occurrence of the noise-induced transition.[5]

In a semigroup formulation of continuous Markov processes,[13] $p_s(x)$ is a weight function which can be interpreted as an invariant measure of the process at hand. Its existence implies, in particular, that the process itself is strongly recurrent (or positive ergodic), so that the probability mass cannot escape beyond the boundaries of a given state space.

This concept is used throughout in subsequent sections, where we study the effect of state-dependent regular perturbations on the evolution of x_t.

3. DETERMINATION OF A CHAOTIC REGIME IN THE MODEL SYSTEM: DETERMINISTIC ANALYSIS

According to numerous studies,[14–16] dissipative nonlinear dynamical systems need not approach stationary or periodic states asymptotically. Instead, for appropriate values of their parameters, they tend toward strange attractors on which the motion is chaotic, i.e., both unpredictable over long times and extremely sensitive to initial conditions.

Various analyses show that this seemingly random behavior is not the stochasticity produced by a large number of degrees of freedom, but results instead from strictly deterministic motion on a fractal. Its is then natural to ask by which observables this type of behavior may be most efficiently characterized. Usually, the presence of chaotic states in a system is determined by the properties of the Fourier spectra of one of the dynamial variables[17] of the system. These spectra present broadband noise, possibly superimposed on discrete peaks. However, such spectra provide practically no information as to the actual nature of the chaotic state to which they relate.

An alternative method has been proposed by Procaccia,[18] who introduced a practical guide to the study of strange attractors based on the measurement of their characteristic fractal dimensions. Chaotic motion can be fully described by an infinite hierarchy of static and dynamic invariants which are observed as appropriate fractal dimensions of the attractor. First in this hierarchy is the familiar Hausdorff dimension $D = d_0$ of the attractor, which measures the exponential rate at which the "strange" structure appears.

Two other, more easily computed invariants are also useful in characterizing the chaotic state. These are the information dimension d_1 (commonly denoted σ) and the correlation exponent d_2 (commonly denoted ν),[18,19] defined as

$$d_1 = \lim_{\varepsilon \to 0} \frac{\langle \ln C_i(\varepsilon) \rangle}{\ln(\varepsilon)} \tag{3.1}$$

$$d_2 = \lim_{\varepsilon \to 0} \frac{\ln \langle C_i(\varepsilon) \rangle}{\ln(\varepsilon)} \tag{3.2}$$

where

$$\langle f(C_i(\varepsilon)) \rangle = \lim_{N \to \infty} \frac{1}{N} \sum_{i=1}^{N} f(C_i(\varepsilon)) \tag{3.3}$$

$$C_i(\varepsilon) = \frac{1}{N} \sum_{j \neq i} \Theta(\varepsilon - |\mathbf{z}_i - \mathbf{z}_j|) \tag{3.4}$$

and Θ is the Heaviside function. $C(\varepsilon) = \langle C_i(\varepsilon) \rangle$ is thus the correlation integral which counts how many pairs of points on the attractor are separated by a distance smaller than ε. For small ε, $C(\varepsilon)$ has been shown[19] to grow like a power

$$C(\varepsilon) \sim \varepsilon^{d_2} \tag{3.5}$$

In the case of deterministic chaos in a system of F degrees of freedom, one finds $d_2 < F$. (In general, the signal from random noise results in $C(\varepsilon) \sim \varepsilon^F$.) The information dimension d_1 governs the exponential rate at which one gains information by measuring the state of the system on the attractor with increasing resolution.[19] The interrelation among d_0, d_1, and d_2 has been established[18] to be of the form

$$d_2 \leqslant d_1 \leqslant d_0 \tag{3.6}$$

where equality holds when the covering of the attractor is uniform.

In conclusion, both the correlation exponent d_2 and the information dimension d_1 provide useful measures of the local structure of a strange attractor. Characterizing the attractor with the exponents d_2 and d_1 rather than with the fractal dimension d_0 also has a definite advantage for experimental applications,[20,21] as the algorithms used to calculate d_2 and d_1 converge efficiently, even with a relatively small number of points $\{\mathbf{z}_i\}$ in a time series.

In practice, the analysis proposed by Procaccia is not carried out directly on the time series $\{\mathbf{z}_i\}$ at hand, which is often only of a single variable, but instead on d-dimensional tuplets $\{\mathbf{z}_i, \mathbf{z}_{i+k}, \ldots, \mathbf{z}_{i+(d-1)k}\}$, the procedure being repeated in larger and larger embedding dimensions until results independent of d are obtained.[18]

Our model dynamic system is defined by the evolution equation

$$\mathbf{z}_{n+1} = \Phi(\mathbf{z}_n, \lambda, \tau) \tag{3.7}$$

$$\mathbf{z}_n = (x_n, \alpha_n, y_n) \tag{3.8}$$

with the flow Φ defined by (1.11), (1.20), and (1.21). Depending on the values of the parameters λ and τ, this flow can shrink the volume in state space and thus dissipate its observable information.

Up to now, we have reported on the influence of rapid stochastic perturbations α_t on the evolution of the state variable x. From the stochastic analysis (Section 2) we know that the process $\{x(t)\}$ defined by Eq. (2.3) is non-Markovian, due to the non-white external fluctuations imposed on α_t. In the next section, we present a further treatment of the dynamics given by the three-dimensional flow $\Phi(x, \alpha, y)$. Its continuous version corresponds to a two-dimensional Markov process described by the pair $\{x_t, \alpha_t\}$ which fulfills the set of stochastic differential equations (2.1) and (2.3).

3.1. Stochastic Character of External Perturbations

When the friction constant γ is fixed and τ tends to zero, λ approaches 1, and α_t becomes the conventional OU process[7] whose stationary probability density is

$$p_s(\alpha) = (\gamma/\pi\sigma^2)^{1/2} e^{-\gamma\alpha^2/\sigma^2} \tag{3.9}$$

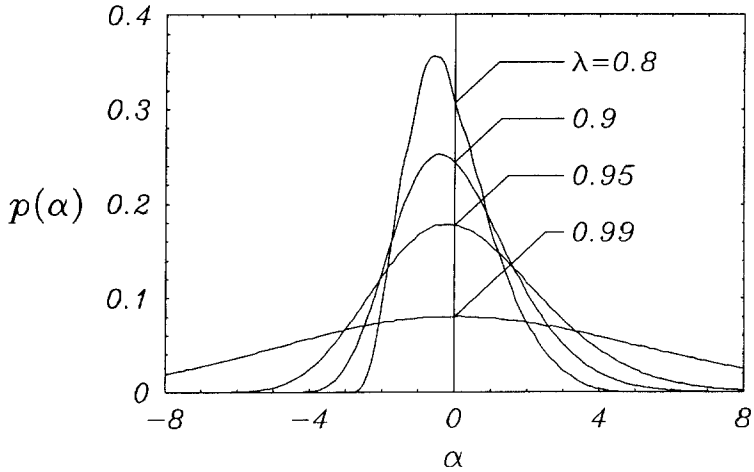

Fig. 1. *A posteriori* probability distribution for α for various values of λ. Each curve represents 10^7 iterations of the map (1.20)–(1.21).

However, for α_n to converge to $\alpha(t)$ with the dynamics predicted by Eq. (1.22) requires that α scale as $\alpha(t) = \tau^{1/2}\alpha_{\lfloor t/\tau \rfloor}$.[7] This is borne out by the following analysis.

In Fig. 1, we present the *a posteriori* probability distribution of α as generated by the map (1.20)–(1.21) for four different values of λ. Each histogram $p(\alpha)$ represents an average over 1000 trajectories, each of 10^4 points. As $\lambda \to 1$, the half-width of the distribution of $\{\alpha\}$ can be seen to increase, and the distributions appear to the naked eye to be approximately Gaussian.

In Table I, we present various statistical parameters of the distribution of α for various values of λ. Each set of statistics represents averages over 1000 trajectories, each of 10^4 points. For each value of λ studied, the mean of the distribution is roughly zero, but the standard error $\sigma_\alpha = \langle (\alpha - \langle \alpha \rangle)^2 \rangle^{1/2}$ grows with increasing λ. In fact, for large λ, $\sigma_\alpha \sim 1/(-\ln \lambda)^{1/2}$, consistent with the scaling requirement imposed by (1.22).

Also given in Table I is the standard error of the mean of the individual trajectories σ_μ. From the central limit theorem, we know that σ_μ should be roughly $\sigma_\alpha / N_T^{1/2}$, where N_T is the number of points in an individual trajectory, provided that each trajectory is sufficiently long so as to sample the entire space. Evidently, increasingly long trajectories must be

Table I. The Mean $\langle \alpha \rangle$, Standard Error σ_α, Dimensionless Measures of the Skewness and Kurtosis γ_3 and γ_4, and Variance of the Mean σ_μ for the α Process (1.20)–(1.21) for Various Values of λ[a]

λ	$\langle \alpha \rangle$	σ_α	γ_3	γ_4	σ_μ
0.1	6.22×10^{-5}	0.708	2.14×10^{-2}	1.54	7.73×10^{-3}
0.2	7.01×10^{-5}	0.718	8.19×10^{-2}	1.63	8.70×10^{-3}
0.3	8.03×10^{-5}	0.739	0.172	1.75	9.94×10^{-3}
0.4	-1.12×10^{-4}	0.768	0.283	1.96	1.17×10^{-2}
0.5	3.60×10^{-4}	0.812	0.400	2.23	1.36×10^{-2}
0.6	1.20×10^{-4}	0.878	0.509	2.55	1.72×10^{-2}
0.7	-2.38×10^{-4}	0.983	0.591	2.88	2.36×10^{-2}
0.8	1.04×10^{-5}	1.17	0.615	3.14	3.62×10^{-2}
0.9	6.24×10^{-5}	1.60	0.535	3.25	7.31×10^{-2}
0.99	1.21×10^{-2}	4.96	0.194	3.07	0.725
0.999	0.224	15.7	7.19×10^{-2}	3.03	6.97
0.9999	0.807	39.7	8.11×10^{-3}	3.01	31.6

[a] For a Gaussian distribution, $\gamma_3 = 0$ and $\gamma_4 = 3$. Note the dramatic increase in both σ_α and σ_μ, as well as σ_α/σ_μ, with increasing λ. These statistics represent averages over 10^3 trajectories, each of 10^4 points.

taken for this condition to be met. In fact, even increasing the length of the individual trajectories by two orders of magnitude was observed to have little effect on the standard error of the mean. Moreover, the study of longer trajectories provided striking examples of the gambler's-ruin scenario, in that a slight preponderance of trajectories to one side of the origin or the other gave rise to large values of both skewness and kurtosis for the entire distribution.

This implies that $\{\alpha_n\}$ approaches its diffusion limit very slowly. Thus, in evaluating Eq. (1.11), we have avoided possible divergences introduced by the perturbations of α by renormalizing the values of α_{n+1} with the standard error σ_α and mean $\langle\alpha\rangle$ calculated directly from the mapping (1.20)–(1.21):

$$\alpha_{n+1} \leftarrow \frac{\alpha_{n+1} - \langle\alpha\rangle}{\sigma_\alpha} \tag{3.10}$$

By making use of Eq. (3.9) as an invariant measure for the diffusion process $\{\alpha(t)\}$, one can easily follow the definition (3.4) to calculate the one-dimensional correlation integral

$$C_1(\varepsilon) = \frac{\gamma}{\pi\sigma^2} \int_{-\infty}^{+\infty} d\alpha \int_{\alpha-\varepsilon}^{\alpha+\varepsilon} e^{-\gamma(\alpha^2+x^2)/\sigma^2}\, dx$$
$$\underset{\varepsilon \to 0}{=} \frac{\varepsilon}{\sqrt{\pi}} \frac{2\gamma}{\sigma^2} \tag{3.11}$$

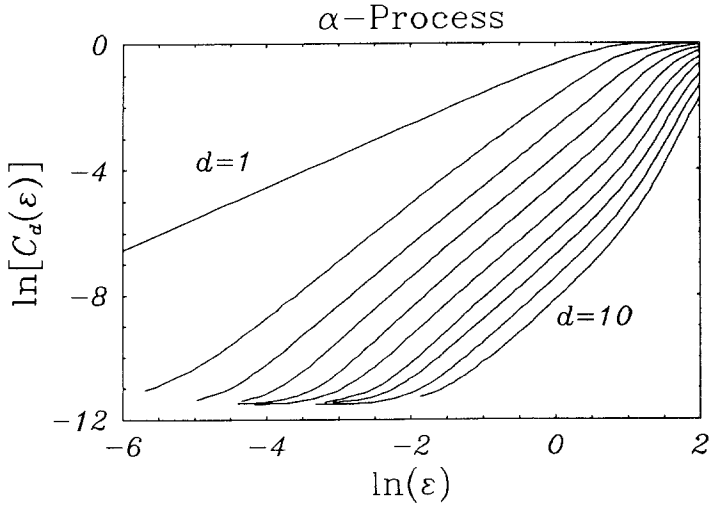

Fig. 2. Correlation integrals of the α process (1.20)–(1.21) for different embedding dimensions d; $\lambda = 0.9$.

Thus, according to (3.2), the correlation exponent should in this limit approach 1. Figure 2 presents the results of numerically calculated $C_d(\varepsilon)$ for the system (1.21) with $\lambda = 0.9$ for embedding dimensions $d = 1, 2, \ldots, 10$. All curves saturate at large values of ε due to the finite size of the attractor and at small values of ε due to the finite size of the data set. $C_1(\varepsilon) \sim \varepsilon$ because the α process is space filling in $d = 1$. In higher embedding dimensions $d > 1$, regions wherein $\ln C_d(\varepsilon)$ is of nearly constant slope $d_2 < d$ appear. However, these regions are not strongly persistent to large embedding dimensions, nor are they present over a wide range of ε for smaller values of λ. This suggests the existence of an underlying structure, but one which cannot be a strange attractor, particularly as the slope of the "scaling regions" of $\ln C_d(\varepsilon)$ remains weakly dependent on d.

Note that $\sigma^2/2\gamma$ is the variance of the process—the time-correlation function for the OU process is $\bar{c}(t-s) = (\sigma^2/2\gamma)\exp(-\gamma|t-s|)$. In the joint limit $\tau_{\text{corr}} \to 0$, $\sigma \to \infty$, taken such that $\sigma^2/\gamma^2 = \text{const} = \bar{\sigma}^2$, the frequency spectrum of the OU process converges to $\bar{\sigma}^2/2\pi$:

$$\lim_{\substack{\gamma \to \infty \\ \sigma \to \infty}} S(\nu) = \lim_{\substack{\gamma \to \infty \\ \sigma \to \infty}} \frac{1}{2\pi} \int_{-\infty}^{+\infty} e^{-i\nu\tau} \bar{c}(\tau)\, d\tau = \frac{\sigma^2}{2\pi\gamma^2} = \frac{\bar{\sigma}^2}{2\pi} \tag{3.12}$$

i.e., the spectrum becomes completely flat. Its correlation function is then given in this limit by a generalized function

$$\bar{c}(\tau) = \bar{\sigma}^2 \delta(\tau) \tag{3.13}$$

and the OU process converges to Gaussian white noise.

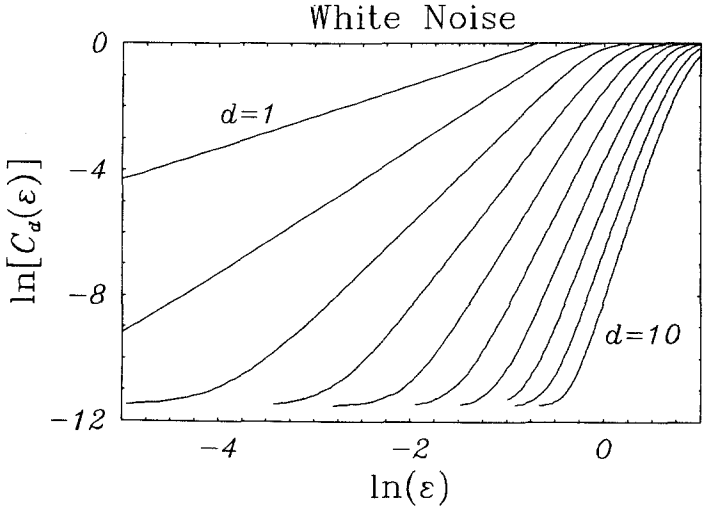

Fig. 3. Correlation integrals for numerically generated, uniformly distributed random numbers (an approximation to white noise).

This limit can also be achieved[5,22] by introducing an appropriate scaling of the OU process [see (2.1)], which in turn leads to a one-dimensional correlation integral

$$C_1(\varepsilon) \underset{\varepsilon \to 0}{=} \frac{\varepsilon}{\sqrt{\pi}} \frac{2}{\sigma^2} \tag{3.14}$$

This would seem to suggest a close similarity between the correlation integrals $C(\varepsilon)$ for both white noise and an OU process.

However, let us point out a notable difference in the behavior of $C_d(\varepsilon)$ for the process (1.21) in comparison to a similarly calculated correlation function of a numerically generated random white noise (Fig. 3). In this case, no region of nearly constant slope (independent of d) appears, and no limiting embedding dimension is reached, so that $C_d(\varepsilon) \sim \varepsilon^d$ as $\varepsilon \to 0$.

In conclusion, we see that although α_n approaches a diffusionlike stochastic process, the transition is not very sharp. Trajectories of α need relatively long runs to uncorrelate and to fill the entire state space.

3.2. Critical Effects Induced by External Perturbations: Evidence of Chaos

Assuming an underlying dynamics of the external parameter α given by Eqs. (1.20)–(1.21), we have numerically calculated histograms of the events x_n whose evolution is governed by Eq. (1.11). For sufficiently long iterates, the histograms "saturate" to an invariant shape (Figure 4) which

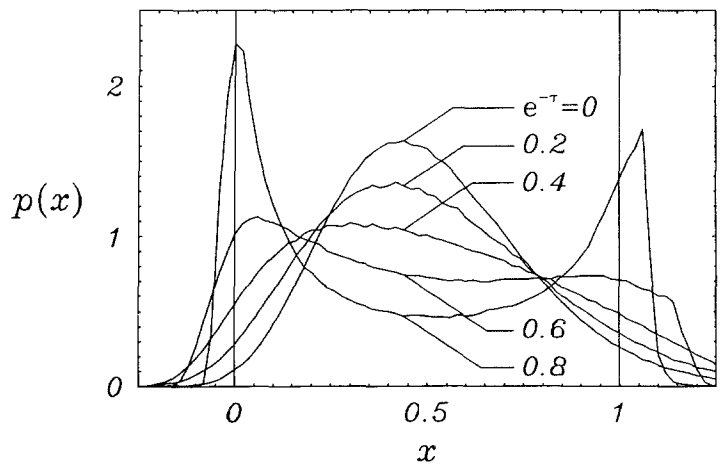

Fig. 4. *A posteriori* probability distribution for x for various values of τ and $\lambda = 0.9$. Each curve represents 500,000 iterations of the map (1.11) with the dynamics of α modeled by (1.20)–(1.21).

represents a stationary probability distribution for the process at hand. The situation displayed is strongly remininscent of the noise-induced transitions discussed in Section 2.

Occupancy of the stationary state $x_s = 1/2$ changes drastically with changing values of τ (we assume that $\gamma = 1/\tau_{\text{corr}}$, the inverse of the correlation time of the process α_t, remains constant). When the time elapsed between subsequent "kicks" in α is long, the stationary probability density is unimodal with a nearly symmetric Gaussian distribution around $x_s = 1/2$. By shortening τ, we arrive at the threshold value τ^*, ($e^{-\tau^*} \simeq 0.6$ for $\lambda = 0.9$), at which point $p_s(x)$ flattens and eventually splits ($\tau < \tau^*$), giving rise to new stationary states $x_{s_1} > 0$ and $x_{s_2} > 1$. Further decreasing of τ leads to the damping of the bottleneck between the maxima, which themselves shift to limiting values of $x_{s_1} = 0$ and $x_{s_2} = 1$, which points also become in the limit the boundaries of the support of x_t. In effect, for sufficiently small values of τ, the transition from one peak to the other becomes a rare event. This suggests that the increasing variability of α favors stabilization of the process x_t near one of the boundaries $x = 0$ or $x = 1$.

A similar conclusion can be drawn by studying diagrams of x_n versus α_n (Figs. 5–8 and 9–12). For sufficiently large values of τ, the most frequently visited parts of the state space (x_n, α_n) correspond to a

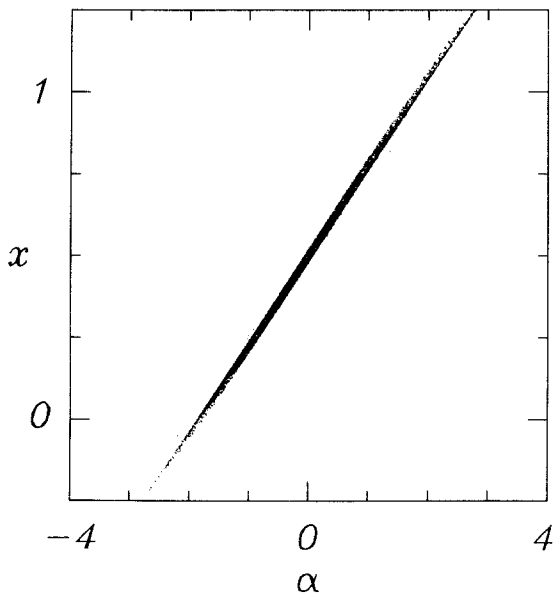

Fig. 5. A diagram of x versus α; $\lambda = 0.9$ and $e^{-\tau} = 0.1$.

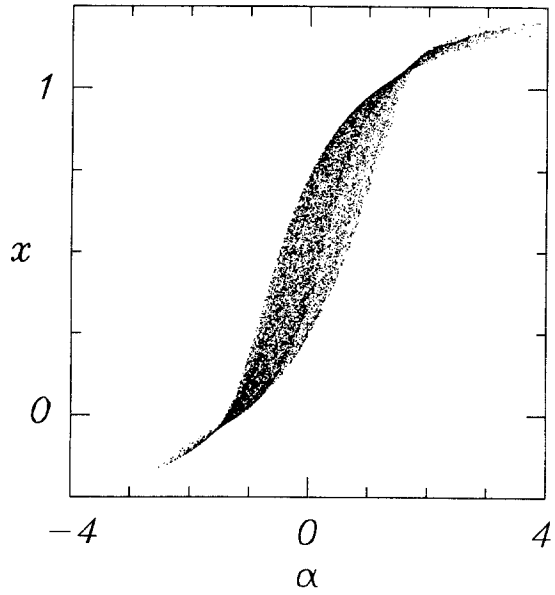

Fig. 6. A diagram of x versus α; $\lambda = 0.9$ and $e^{-\tau} = 0.6$.

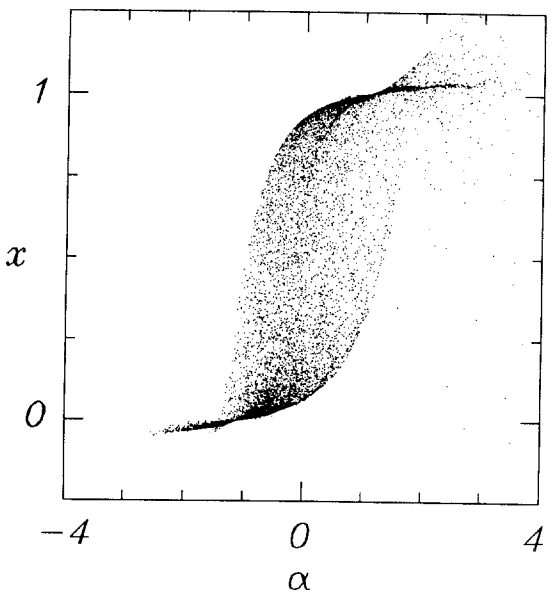

Fig. 7. A diagram of x versus α; $\lambda = 0.9$ and $e^{-\tau} = 0.9$.

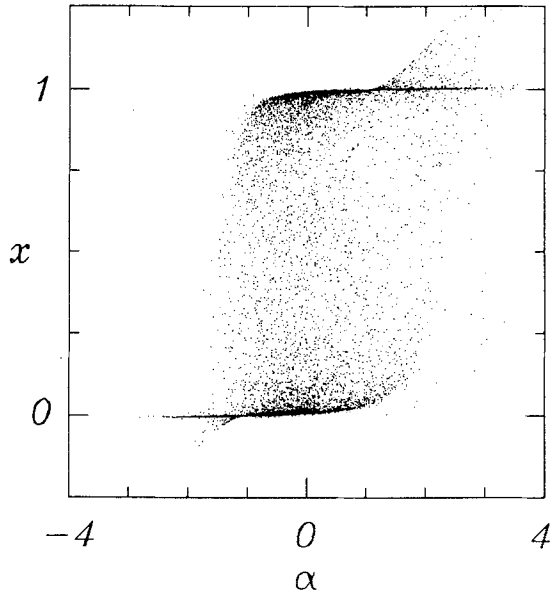

Fig. 8. A diagram of x versus α; $\lambda = 0.9$ and $e^{-\tau} = 0.99$.

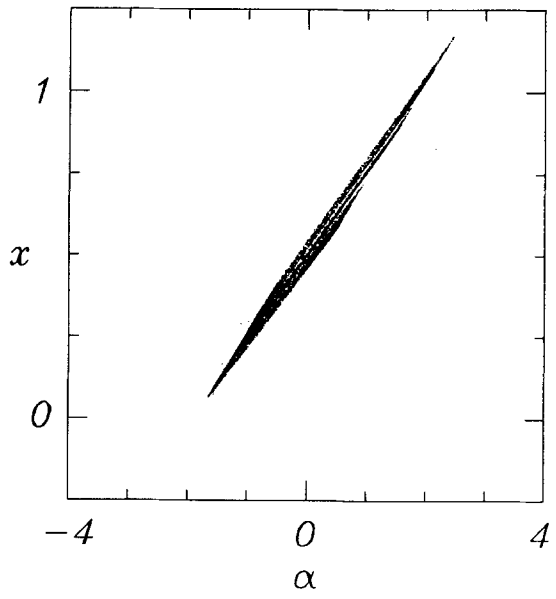

Fig. 9. A diagram of x versus α; $\lambda = 0.5$ and $e^{-\tau} = 0.1$.

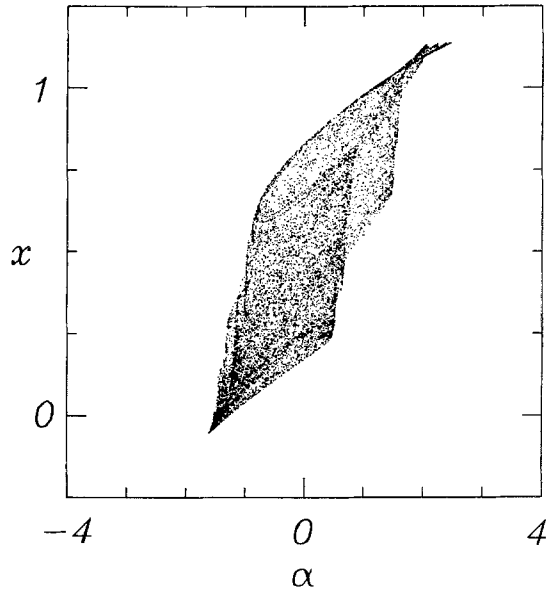

Fig. 10. A diagram of x versus α; $\lambda = 0.5$ and $e^{-\tau} = 0.6$.

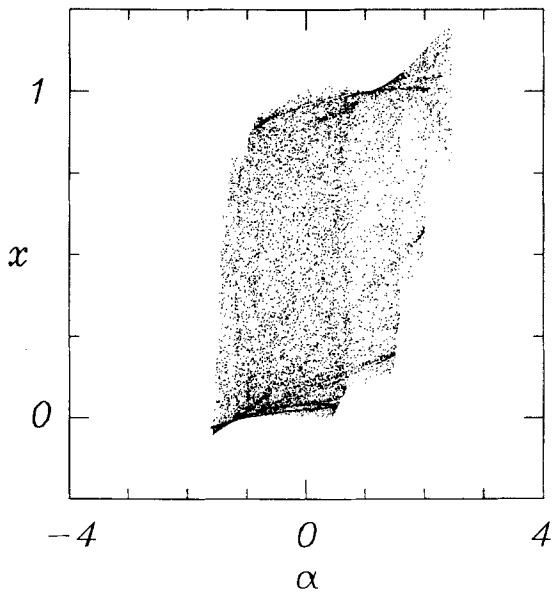

Fig. 11. A diagram of x versus α; $\lambda = 0.5$ and $e^{-\tau} = 0.9$.

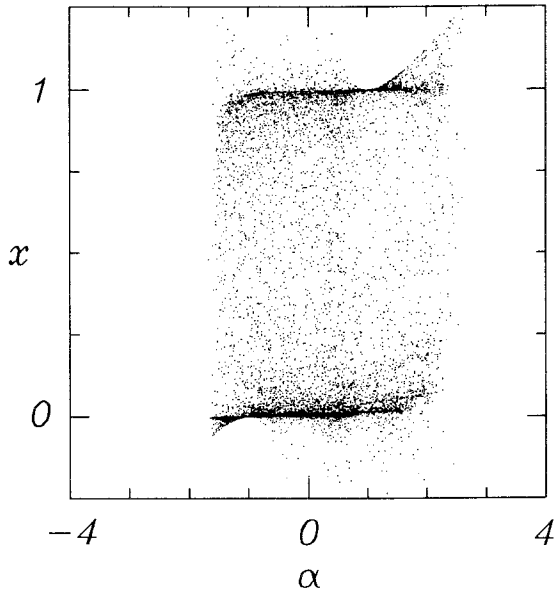

Fig. 12. A diagram of x versus α; $\lambda = 0.5$ and $e^{-\tau} = 0.99$.

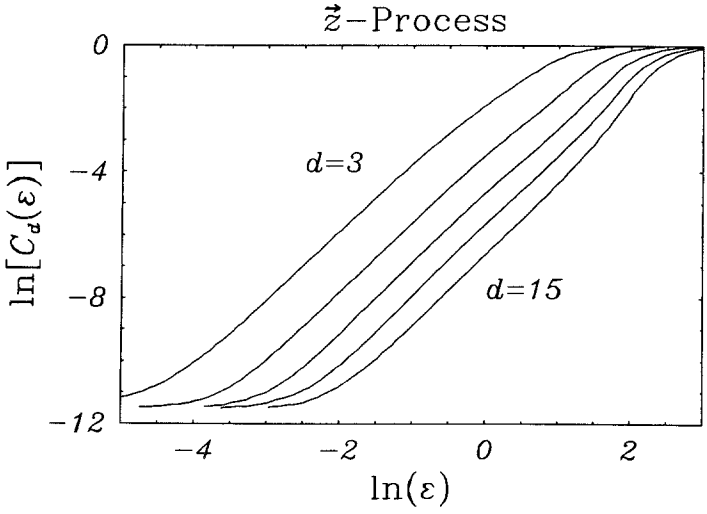

Fig. 13. Correlation integrals of the **z** process [(1.11), (1.20)–(1.21)] for different embedding dimensions d; $\lambda = 0.9$ and $e^{-\tau} = 0.7$.

Table II. The Procaccia Correlation Exponent d_2 for the z Process[a]

λ	$e^{-\tau}=0.1$	$=0.3$	$=0.5$	$=0.7$	$=0.9$
0.1	1.46	1.64	1.84	2.03	2.11
0.3	1.56	1.69	1.87	2.07	2.13
0.5	1.71	1.80	1.95	2.13	2.22
0.7	1.86	1.93	2.06	2.22	2.30
0.9	1.70	1.88	2.05	2.24	2.30

[a] These values represent averages over least-squares fits to $\ln C_d(\varepsilon)$ for $\ln \varepsilon \in (-10, -8)$ for $d = 3, 6, \ldots, 15$.

neighborhood of the diagonal $x_n = \alpha_n$. Rapidly fluctuating α ($\tau \to 0$) generates a hysteresis of states in the space $x \times \alpha$ whose width broadens for smaller values of τ (Figs. 6–8).

As τ decreases, the region of atraction changes drastically, until in the limit it consists (Fig. 8) of two branches of favored x values in the vicinity of the boundaries $x = 0$ and $x = 1$. The smaller τ becomes, the rarer is the switching of the system from one of the branches to the other. For even smaller values of τ (not shown), the two branches become sharp, horizontal lines whose projections overlap in the center of the figure, there being almost no events with x values in the open interval (0, 1).

The significance of the correlation time of external perturbations can be visualized by the use of analogous diagrams (Figs. 9–12) for different values of λ. Figures 9–12 display variability in the region of attraction for the same series of τ values as in the cases described above, from which the only difference is that now $\lambda = 0.5$, which expresses a different choice of correlation time $\tau_{\text{corr}} = 1/\gamma$.

Table III. The Information Dimension d_1 for the z Process[a]

λ	$e^{-\tau}=0.1$	$=0.3$	$=0.5$	$=0.7$	$=0.9$
0.1	1.51	1.69	1.89	2.08	2.10
0.3	1.60	1.73	1.91	2.10	2.18
0.5	1.74	1.84	1.98	2.17	2.25
0.7	1.91	1.99	2.11	2.28	2.38
0.9	1.87	2.04	2.21	2.39	2.46

[a] These values represent averages over least-squares fits to $\langle \ln C_d(\varepsilon) \rangle$ for $\ln \varepsilon \in (-10, -8)$ for $d = 3, 6, \ldots, 15$.

Shorter values of τ_{corr} imply a more complex evolution of x (see, e.g., Fig. 7, $1/\gamma = 1$; and Fig. 11, $1/\gamma \simeq 0.15$) with a visibly deterministic character: The orbit of x_n seems to fall onto a low-dimensional attractor.

This conclusion is confirmed by calculations of the correlation integral for the process $\mathbf{z}_n = (x_n, \alpha_n, y_n)$. A plot of $\ln C_d(\varepsilon)$ versus $\ln \varepsilon$ (Fig. 13) exhibits the scaling region $d_2 = \text{const}$, which persists even in higher embedding dimensions. As the process $\mathbf{z}_n$ is itself three dimensional, we have studied embedding dimensions $d = 3, 6, \ldots, 15$. All curves saturate at large values of ε due to the finite size of the attractor and at small values of ε due to the finite size of the data set.

We have carried out the Procaccia analysis for a number of values of λ and τ for both the correlation exponent d_2 and the information dimension d_1. Our results are summarized in Tables II and III.

It is interesting to note that the phenomenon disappears, however, when a similar analysis is performed on the projection of the process $\mathbf{z}_n$ on the state space of x alone. The results obtained are similar to those seen for the α process (Fig. 2). Although we detect to particular underlying "strange" structure of the underlying attractor, recurrence plots (x_n, x_{n+1}) (Figs. 14–16) clearly indicate the presence of strong "time correlations" of x_n. These illustrations also depict the continuous passage of the process x_t from deterministic to diffusive behavior as controlled by a sequence of decreasing values of τ/τ_{corr}.

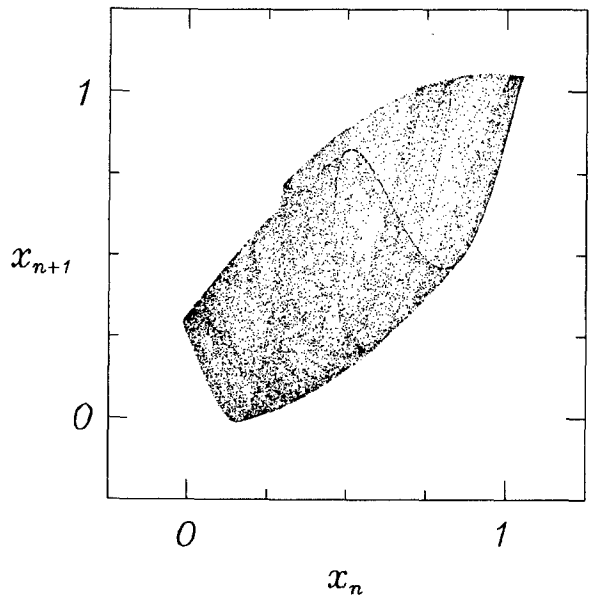

Fig. 14. Recurrence plot of the x process; $e^{-\tau} = 0.7$ and $\lambda = 0.1$, or $\tau = 0.36$ and $\tau/\tau_{corr} = 2.3$.

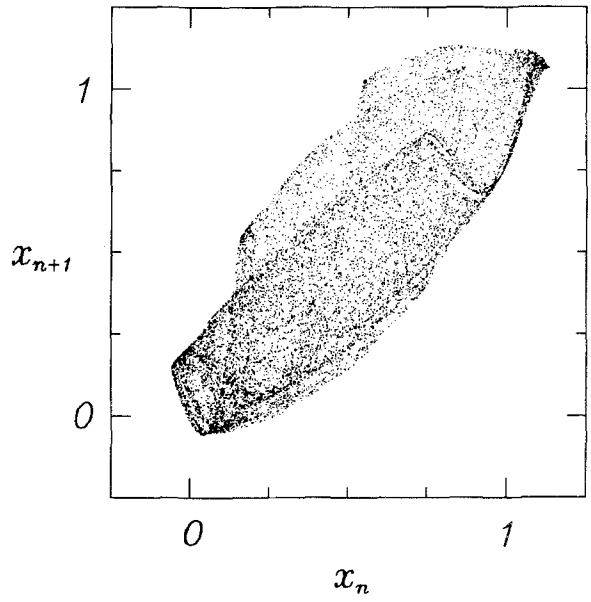

Fig. 15. Recurrence plot of the x process; $e^{-\tau} = 0.7$ and $\lambda = 0.5$, or $\tau = 0.36$ and $\tau/\tau_{corr} = 0.69$.

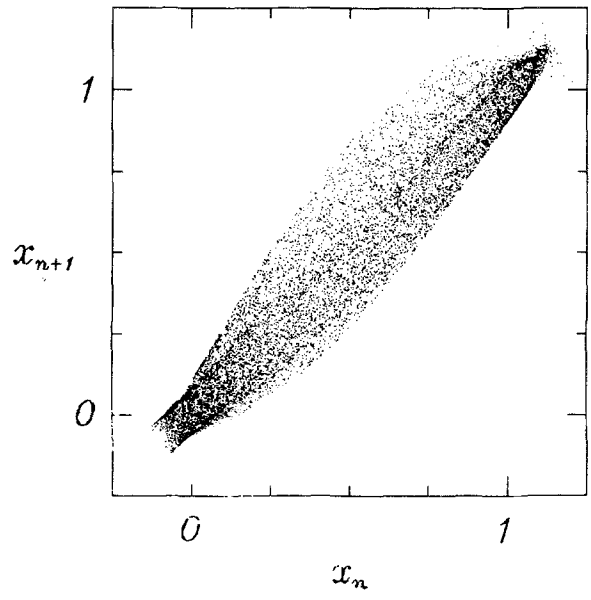

Fig. 16. Recurrence plot of the x process; $e^{-\tau} = 0.7$ and $\lambda = 0.9$, or $\tau = 0.36$ and $\tau/\tau_{corr} = 0.11$.

Let us also note that Markovian character of a given dynamics does not exclude its deterministic nature. In fact, the Markovian property is generic to deterministic processes.[23] Any isolated physical system can be described as a Markov process whose components are all the microscopic variables of the system. Its motion in phase space would then be given by a fully deterministic, and therefore Markovian, flow.

This is the case of the dynamic system analyzed in this paper and defined by the vector $\mathbf{z}_n$ [see (3.7) and (3.8)]. Its emerging chaotic behavior thus has a purely "deterministic" character. On the other hand, a projection of $\mathbf{z}_n$ onto a lower-dimensional state space produces a non-Markovian process whose properties, even in the case of regularly disturbed external parameters, can lead to a stochastic evolution.

4. CONCLUSIONS

We have described a dynamical system whose time evolution depends on externally perturbed model parameters. It was observed that inclusion of state-dependent perturbations can induce a variety of phenomena which can have either a chaotic or stochastic nature.

After reviewing the well-known properties of the stochastic continuous version of the model (Section 2), we analyzed its deterministic analog (Section 3). To distinguish between perturbation-induced chaotic and stochastic behaviors, we used the concept of the correlation exponent proposed by Grassberger and Procaccia.[18]

The possibility of the existence of fractal attractors and/or diffusive motion has been pointed out by studying the sensitivity of a given dynamics to the strength, frequency, and time correlations of external perturbations.

It has been shown that in the limit case, when the dynamics of the perturbations converge to a stationary Gaussian diffusion process, the long-time behavior of the model system coincides with the predictions afforded by a stochastic analysis.

In particular, the implications of rapidly varying perturbations have been expounded by evidence of effects similar to noise-induced transitions.

ACKNOWLEDGMENTS

The contributions of E.G.-N. and A.K. were supported by the Polish Research Program CPBP 01.03.

REFERENCES

1. J. F. Crow and M. Kimura, *An Introduction to Population Genetics Theory* (Harper, New York, 1971).
2. T. D. Rogers, *Prog. Theor. Biol.* **6**:91 (1980).
3. S. Karlin and H. M. Taylor, *A Second Course in Stochastic Processes* (Academic Press, New York, 1981).
4. P. Collet and J.-P. Eckman, *Iterated Maps on the Interval as Dynamical Systems* (Birkhäuser, Boston, 1981).
5. W. Horsthencke and R. Lefever, *Noise-Induced Transitions* (Springer-Verlag, Berlin, 1984), and references therein.
6. A. Fulinski, *Phys. Lett.* **126A**:84 (1987); E. Gudowska-Nowak and J. Krawczyk, unpublished.
7. C. Beck and G. Roepstorff, *Physica* **145A**:1 (1987).
8. P. Billingsley, *Convergence of Probability Measures* (Wiley, New York, 1968).
9. G. Roepstorff and D. Mayer, *J. Stat. Phys.* **31**:309 (1983).
10. C. J. Thompson and R. Ter Bush, *Biopolymers* **10**:961 (1971).
11. N. S. Goel, *Biopolymers* **6**:55 (1968).
12. A. M. Ziff, E. Gulari, and V. Barshad, *Phys. Rev. Lett.* **56**:2553 (1986).
13. W. Feller, *An Introduction to Probability Theory and Its Applications*, Vol. II (Wiley, New York, 1957).
14. D. Ruelle and F. Takens, *Commun. Math. Phys.* **20**:167 (1971).
15. E. Ott, *Rev. Mod. Phys.* **53**:655 (1981).
16. J.-P. Eckmann, *Rev. Mod. Phys.* **53**:643 (1981).
17. H. L. Swinney and J. P. Gollub, *Phys. Today* **31**:41 (1978).
18. P. Grassberger and I. Procaccia, *Physica* **9D**:189 (1983); I. Procaccia, *Physica Scripta* **T9**:40 (1985).
19. P. Grassberger and I. Procaccia, *Phys. Rev. Lett.* **50**:346 (1983).
20. J. Guckenheimer and G. Buzyna, *Phys. Rev. Lett.* **51**:1348 (1983); G. O. Williams and H. L. Frisch, unpublished.
21. B. Malraison, P. Atten, P. Berge, and M. Dubois, *J. Phys.* (Paris) **44**:L897 (1983).
22. C. van den Broeck, *J. Stat. Phys.* **31**:467 (1983).
23. N. G. van Kampen, *Stochastic Processes in Physics and Chemistry* (North-Holland, Amsterdam, 1981).